CHIN. PHYS. LETT. Vol. 34, No. 9 (2017) 094201

High-Order-Harmonic Generation from a Relativistic Circularly Polarized Laser Interacting with Over-Dense Plasma Grating *

Xia-Zhi Li(李夏至)[1], Hong-Bin Zhuo(卓红斌)[1,2,3**], De-Bin Zou(邹德滨)[1**], Shi-Jie Zhang(张世杰)[1], Hong-Yu Zhou(周泓宇)[1], Na Zhao(赵娜)[1], Yue Lang(郎跃)[1], De-Yao Yu(余德尧)[1]

[1]*College of Science, National University of Defense Technology, Changsha 410073*
[2]*IFSA Collaborative Innovation Center, Shanghai Jiao Tong University, Shanghai 200240*
[3]*Institute of Applied Physics and Computational Mathematics, Beijing 100094*

(Received 24 May 2017)

The simple surface current model is extended to study the generation of high-order harmonics for a relativistic circularly polarized laser pulse interacting with a plasma grating surface. Both exact relativistic electron dynamics and optical interference of surface periodic structure are considered. It is found that high order harmonics in the specular direction are obviously suppressed whereas the harmonics of the grating periodicity are strongly enhanced and folded into small solid angles with respect to the surface direction. The conversion efficiency of certain harmonics is five orders of magnitude higher than that of the planar target cases. It provides an effective approach to generate a coherent radiation within the so-called 'water window' while maintaining high conversion efficiency and narrow angle spread.

PACS: 42.65.Ky, 42.79.Dj, 28.52.Av, 28.52.−s DOI: 10.1088/0256-307X/34/9/094201

High-order-harmonic generation (HHG) and attosecond science continue to be rapidly evolving areas of research and applications, including high density plasma physics, solid-state physics and x-ray imaging.[1−4] Among the available harmonic sources, the brightness and intensity of the radiation generated by synchrotron and free electron laser are seriously limited by the number and quality of electron sources.[5] In contrast to these electrons obtained from the conventional accelerators, plasma can provide a large number of free electrons required for the efficient interaction with the laser fields.[6,7] It is a promising alternative to obtain high-order harmonics (HHs) from the relativistic motion of the dense electrons in the laser plasma interaction[8,9] as new ultrafast attosecond pulse sources. Several works are devoted to the generation of intense laser-driven high order harmonic sources, including in gas targets[10−12] or in over dense plasmas.[13] In particular, high bright HHs have been generated from the flat solid targets obliquely irradiated by linearly polarized (LP) laser pulse at relativistic intensities in both the simulations[14] and experiments.[15] In these regimes, the plasma acts as an oscillating mirror to the incident field, leading to a periodic temporal distortion of the reflected waveform and thus the harmonic is generated in the specular reflection of the laser pulse.[15] In the time domain, the HHs from the solid targets show the form of a train of attosecond pulses that can be separated from the laser fundamentally reflected from the bulk target surface for some potential applications.[16−18]

Recently, HHs generated from a solid target normally irradiated by a short-pulse ultra-intense circularly polarized (CP) laser were theoretically studied by Yu *et al.*[19] It shows that a considerable part of the scattered energy is in the form of higher order harmonics in the nonlinear scattering from the movement of relativistic electrons for a laser with a sufficient intensity ($I_0 \sim 6.25 \times 10^{18}/\lambda_0^2$, I_0 is the laser intensity in units of W/cm^2 and λ_0 is the laser wavelength in units of μm). Meanwhile, for high order modes, both the intensity and the angle of the radiation peak at the direction nearly perpendicular to the incident light. However, the conversion efficiency from laser to high harmonics is very low (generally $<10^{-7}$),[19] which is a large challenge for the actual applications.

In this Letter, a novel configuration of a high intensity circularly polarized laser pulse interacting with periodically modulated grating targets is proposed to efficiently enhance the HHs along the target surface direction. A simple surface current model[20] is adopted to describe the harmonic generation. The result indicates that HHs in the reflection direction are considerably weakened but HHs in the direction nearly parallel to the target surface are strongly enhanced with their wavelengths equal to the integer multiple of the grating periodicity. The enhanced efficiency of certain wavelength radiation is about five orders higher than that of the planar target case. This enhancement effect is attributed to the interference effect of the periodic grating on these harmonics generated on the surface, which provides us with an effective approach to optimize the spectral and spatial components of harmonics emitted from plasma surfaces. Moreover, HHs are separated from the laser at the fundamental frequency perpendicularly reflected from the plasma

*Supported by the National Natural Science Foundation of China under Grant Nos 11375265, 11475259 and 11675264, the National Basic Research Program of China under Grant No 2013CBA01504, and the Science Challenge Project under Grant No JCKY2016212A505.
**Corresponding author. Email: hongbin.zhuo@hotmail.com; debinzou@126.com.
© 2017 Chinese Physical Society and IOP Publishing Ltd

target surface while maintaining a short duration and narrow angle spread.

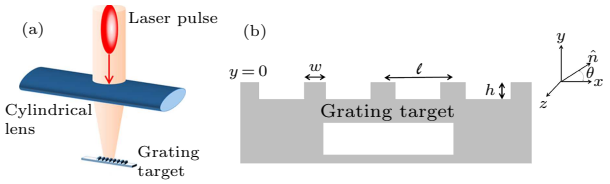

Fig. 1. Schematics of the laser grating-target interaction. (a) A relativistic circularly polarized laser beam is reshaped into a linear pulse by a cylindrical lens. The reshaped linear laser normally impinges on the grating surface located in the focus plane with its electric field polarized along the e_x and e_z axes. (b) The surface $y = 0$ is the interface of tooth and vacuum. Here l, h and w are the grating periodicity, height and width of the tooth, respectively, and θ is the observation angle, namely, the emission angle in the x–y plane.

The proposed configuration for HHG is illustrated in Fig. 1(a). A circularly polarized laser pulse is reshaped through a cylindrical lens and focused into a 1D linear spot and impacts on a solid density plasma grating fixed in the focal panel of the lens. The corresponding parameters are denoted in Fig. 1(b), the surface $y = 0$ is the interface of tooth and vacuum. Here l, h and w are the grating periodicity, height and width of the tooth, respectively. We consider a normal incidence of a relativistic CP laser pulse propagating along the y-axis with the wavelength of λ_0. The parametric condition of the grating here satisfies the relationship of $w \ll l \ll \lambda_0$. Thus we can neglect the optical effect of the grating on the spatial distribution of the transmitted and incident fields on the zeroth order approximation.[21] When the laser electric field is much stronger than that of the atom nucleus, field ionization by barrier suppression is dominant in the femtosecond timescale.[22] For simplicity, we assume that the grating structure is instantly ionized and its density profile keeps constant within a short interaction time. The density profile of the teeth remains steplike, which is n_0 for $y < 0$ and 0 for $y \geqslant 0$, respectively. At $y > 0$, the incident and reflected laser fields are given as $a_{\rm i}(y,t) = a_0(\hat{x} + i\hat{z})e^{(j\omega_0 t - k_0 y)}$ and $a_{\rm r}(y,t) = Ra_0(\hat{x} + i\hat{z})e^{(j\omega_0 t + k_0 y)}$, where $a_0 = eE_0/m_{\rm e}\omega_0 c$ is the normalized field peak amplitude, ω_0 is the laser fundamental frequency, c is the speed of light, R is the reflecting factor, and e and $m_{\rm e}$ are the electron charge and rest mass, respectively. As the density n_0 of plasma grating target is far beyond the critical density $n_{\rm c}$, the laser can only penetrate into the plasma surface within a skin-layer depth (far less than the laser wavelength). Therefore, the laser absorption is much less than the total laser energy and the reflecting factor is $R \sim 1$. At the interface between target and vacuum, the boundary condition can be simply described as $a_{\rm t}(o,t) = a_{\rm i}(o,t) + a_{\rm r}(y,t) \approx 2a_{\rm i}(o,t)$, where $a_{\rm t}$ is the field for the transmitted waves. In the limit of $n_0 \to \infty$, the transmitted wave can also be represented by a surface current $j(0,t)$, which could be given by $(4\pi/c)j(0,t) = \nabla \times \nabla \times a_{\rm t}(o,t)$. We can easily obtain $j(0,t) = (m_{\rm e}\omega_0 c^2/2\pi e)\gamma\beta(t)$, where $\beta(t) = ea_{\rm i}/\gamma m_{\rm e}c$ is the normalized electron quiver velocity under the circularly polarized laser force and $\gamma = (1-\beta^2)^{-1/2} \approx (1+a_0^2)^{1/2}$. Taking account of the grating periodic structure, the current density along the grating surface can be described as the sum of the each-tooth current,[20] i.e.,

$$j_{\rm total}(x,t) = \sum_{m=1}^{L/l} \sigma(x - ml) j(0,t), \tag{1}$$

where L is the grating length inside the laser spot, and m is the tooth index.

For an electron executing a circular path motion in the CP laser fields, the radiation spectrum is discrete, composed of the harmonics of the laser frequency. Thus the total radiation power per unit solid angle of the nth harmonic from a current source can be expressed as[19]

$$\frac{dP_n}{d\Omega} = \frac{n^2\omega_0^2}{8\pi^3 c^3}\Big|\int d^3x \exp(-ink_0 n \cdot x \int_0^{2\pi} d\tau G_n)\Big|^2, \tag{2}$$

where $n = \{e_x \cos\theta\cos\varphi + e_z \cos\theta \sin\varphi + e_y \sin\theta\}$ is the emission direction of HHG, θ is the observation angle in respect to the e_y-direction, $G_n = n \times n \times j_{\rm total}(x,t)\exp[in(\tau - k_0 n \cdot \Delta)]$, x is the coordinate vector of the source, $\tau = \omega_0 t$, $k_0 = \omega_0/c$, $\Delta(x,\tau) = \int_0^\tau v[x,\tau']d\tau'$ is the displacement, and $x + \Delta$ is the instantaneous location of the source. For a CP laser field, the displacement of an electron can be described as $\Delta = \beta c/\omega_0(e_x \cos\tau - e_z \cos\tau)$. Substituting $j_{\rm total}(x,t)$ and Δ in Eq. (2), we obtain

$$\frac{dP_n}{d\Omega} = \Big(\frac{\gamma m_{\rm e}\omega_0 c}{2\pi c}\Big)^2 F_n(\omega_0,\theta)K_n(\theta). \tag{3}$$

Physically, the term $K_n(\theta)$ describes the radiation generated from a single electron oscillating in the circularly laser field,[19] which is written as

$$K_n(\theta) = \frac{n^2 e^2 \omega_0^2}{2\pi c}[\cot^2\theta J_n^2(n\beta\sin\theta) + \beta^2 {J'_n}^2(n\beta\sin\theta)], \tag{4}$$

where J_n and J'_n are the nth-order Bessel function and its derivative, and $F_n(\omega_0,\theta)$ represents the collective effect of the periodic grating on the excited radiation field as

$$F_n(\omega_0,\theta) = |\sum_{m=1}^{L/l} e^{imnlk_0\cos\theta}|^2 = \frac{\sin^2(\frac{n\omega_0 L\sin\theta}{2c})}{\sin^2(\frac{n\omega_0 l\sin\theta}{2c})}. \tag{5}$$

For the case of $L \gg l$, the interference factor degenerates into another simple form

$$F_n(\omega_0,\theta) \to \sum_{m\neq 0} \frac{n\omega_0 L}{|m|l}\delta(n\omega_0 - \omega_m), \tag{6}$$

and

$$n\omega_0 = \omega_m = \frac{2\pi mc}{l\sin\theta}. \tag{7}$$

According to Eq. (3), the HHs emission from a grating target is a result of coherent enhancement of the radiation originating from each grating's protuberance. The spectral and angular distribution in the far-field region are modulated by the constructive interference of the emitted waves.

Figures 2(a) and 2(b) show the angular dependence of $K_n(\theta)$ for $a_0 = 0.5$ and $a_0 = 3.0$, respectively. In the low-intensity limit, the main portion of the observed radiation concentrates on the low-order harmonic components. The major part of the radiated energy is almost of the same frequency as the laser, with a wide angular spread peaking at the specular direction as shown in Fig. 2(a). For a relativistic laser intensity of $a_0 = 3.0$, most of the radiated energy is concentrated in higher harmonics and its spatial distribution is obviously away from the perpendicular direction of the surface. The radiation at the laser fundamental frequency still peaks at the perpendicular direction of the target surface, but turns to be comparatively weak. With the increase of the harmonic order, the angular distribution of the harmonic components progressively shifts toward the electron orbit plane, together with an increasingly sharp peak, as can be seen for the 48th harmonics component in Fig. 2(b).

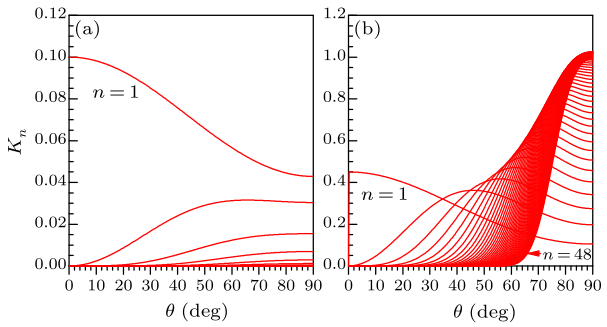

Fig. 2. The angular distribution of $K_n(\theta)$ for $a_0 = 0.5$ (a) and $a_0 = 3.0$ (b). Here $K_n(\theta)$ is normalized by $e^2\omega_0^2/2\pi c$. In (a) n = 1–5 are shown from upper to lower. In (b) n = 1–48 are shown from left to right.

The term $F_n(\omega_0, \theta)$ accounts for the optical interference of the surface periodic structure on the nth order laser harmonic power. It acts as a frequency modulator to enhance or suppress the harmonics power into a certain observation angle. Figure 3 shows the angular distribution of $F_n(\omega_0, \theta)$ for the harmonics with different number n. The grating parameters chosen here are $l = \lambda_0/4$ and $L = 24l = 6\lambda$. As shown in Fig. 3(a), for the fundamental laser, i.e., $n = 1$, F_1 peaks at $\theta = 0°$ and decreases rapidly with the increase of the angle. For high order harmonics, several sharp peaks are observed at individual angles in Figs. 3(b)–3(d). According to Eq. (5), the optimal angles of F_n are well predicted by $\theta_m = \arcsin(m\lambda_0/nl)$, where m is an integer. At $\theta_m = \pi/2$, the condition for the harmonic enhancement is given by $\lambda_0/n = l/m$. Thus in the direction parallel to the target surface, only the harmonics of the grating periodicity are strongly enhanced due to the interference effect of the grating, as can be seen for the 4th, 12th, and 48th harmonics components in the plot of Figs. 3(b)–3(d). Moreover, a common plateau around the peak angle of $\theta = 90°$ is observed for these matched harmonics. Except for $\theta = 90°$, it should be mentioned that there are some peaks at different angles in Figs. 3(c) and 3(d). However, they are extremely narrow and can be neglected compared with the main peak near $\theta = 90°$ when integrating in the whole space. The angular distribution of the radiation power suggests that most of the matched harmonic energies can be folded into small solid angles with respect to the surface direction.

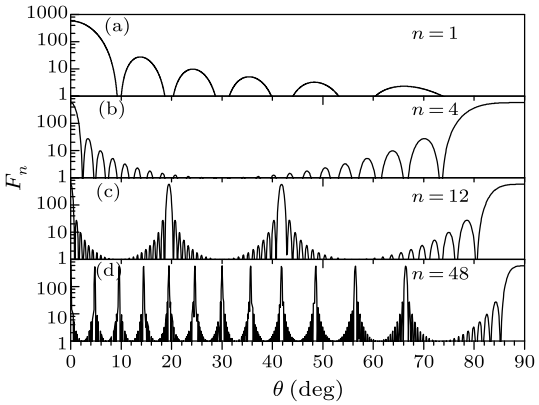

Fig. 3. Diffraction factor $F_n(\omega_0, \theta)$ for different harmonic orders n. The grating parameters are $l = \lambda_0/4$ and $L = 24l = 6\lambda_0$.

The angular distribution of the radiation power in far field is determined by K_n and F_n, where K_n is a radiation from a single electron oscillating and F_n accounts for the optical interference of surface periodic structure on the far-field radiation. Since $K_1(\theta)$ and $F_1(\theta)$ reach the maximum at $\theta = 0°$, the harmonic at the fundamental frequency $n = 1$ is concentrated in the specular direction. However, for high-order harmonics suitably matches a harmonic of the grating periodicity, both $K_n(\theta)$ and $F_n(\theta)$ peak at $\theta = 90°$ and concentrate in the surface direction with a narrow angular spread, such as the harmonics $n = 12$ and $n = 48$ in Figs. 4(a) and 4(b). For no matched harmonics, i.e., $n \neq 4m$, the peaks of $K_n(\theta)$ and $F_n(\theta)$ are not overlapped. The harmonic power deviates from the surface direction with different angles and lower amplitudes. As shown in Figs. 4(a) and 4(b), the 14th and 50th harmonic power peak at 60° and 73°, respectively, and both vanish at $\theta = 90°$. We compare the radiation power emitted from the grating target with that of the usual planar target. In the latter case, $F_n(\omega_0, \theta)$ in Eq. (3) is replaced by the Fraunhofer diffraction of rectangular apertures as[23]

$$F_n(\omega_0, \theta) = \frac{\sin^2(nk_0 L \sin\theta/2)}{nk_0 L \sin\theta/2}. \tag{8}$$

As shown in Figs. 4(c) and 4(d), the power of the 12th, 14th, 48th and 50th harmonics for the planar target case is almost two orders of magnitude lower than that of the grating target cases. Meanwhile, all

harmonics show a relatively wide angular spread but vanish at $\theta = 90°$. Based on our model, the difference between the grating and planar targets is a straight result from the different optical interference of the plasma surface structure. In Ref. [24] the interaction of an LP laser and plasma target has been investigated in our previous work. We find that the power of the radiation at the 48th order harmonic driven by the CP incident laser is much higher, which is up to 42 times, than that driven by the LP laser. Such a considerable enhancement is due to the spatial match of peak values of $K_n(\theta)$ and $F_n(\omega_0, \theta)$ alongside the target surface. For the CP incident condition, both $K_n(\theta)$ and $F_n(\omega_0, \theta)$ peak at the target surface whilst $K_n(\theta)$ of LP laser deviates from the target surface and peaks at $\sim 20°$.

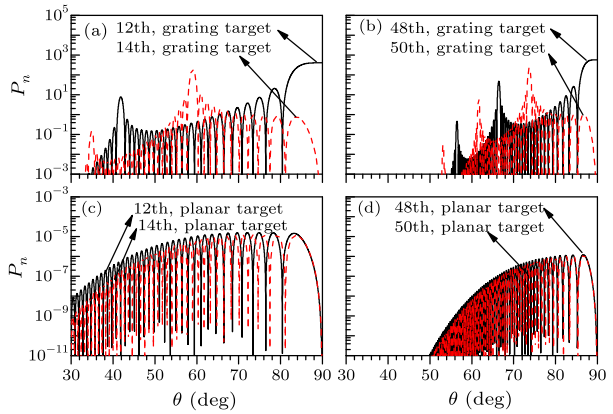

Fig. 4. The angular distribution of the radiation power P_n versus different harmonic orders from the grating surface for $a_0 = 3.0$ [(a) 12th and 14th; (b) 48th and 50th] and the planar target [(c) 12th and 14th; (d) 48th and 50th]. The parameters of the grating target are the same as those in Fig. 3

The harmonic emission can be described as the nonlinear scattering of the light from the plasma in terms of the differential cross section for light scattered per unit solid angle at the nth harmonic

$$\frac{dP_n}{d\Omega} = I\frac{d\sigma_n}{d\Omega}, \tag{9}$$

where σ_n is the scattering cross section, and $I = (c/4\pi)|m_e\omega_0 c a_0/e|^2$ is the laser intensity. Based on Eqs. (3) and (9), we can obtain $\sigma_n = \int (dP_n/Id\Omega)d\Omega$. The conversion efficiency is defined as $\eta_n = \sigma_n/S$, where S is the interaction area of the laser and grating target. In the one-dimensional approximation, it is simplified to $\eta_n = \int (dP_n/Id\Omega)d\theta/L_{\min}$, where $L_{\min} = \min(L, d_0)$ is the minimum interaction length, and d_0 is the diameter of the focused laser spot. The conversion efficiencies of the 12th and 48th harmonic components versus the laser amplitude a_0 are plotted in Fig. 5. For the grating target cases, the conversion efficiency η_n increases rapidly from $a_0 = 0.5$ and roughly saturates when $a_0 \geqslant 2.0$. The peak conversion efficiency for two such harmonics is close to 10^5, almost five orders higher than that of the planar target case. As shown in Fig. 6, for fixed laser intensities the conversion efficiency η_n in the grating target cases falls off monotonically with harmonics number n. The trend of this decrease is much steeper for weakly relativistic laser $a_0 = 1$, but turns to flatten with increasing the laser intensity.

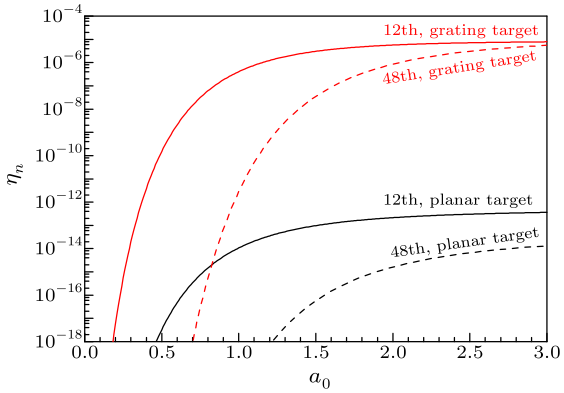

Fig. 5. The conversion efficiencies of 12th and 48th harmonics versus laser strength a for the planar surface (solid lines) and the grating surface (dash lines). The parameters of the grating are the same as those in Fig. 3.

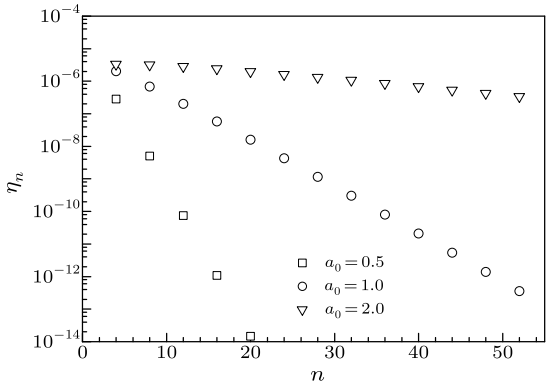

Fig. 6. Conversion efficiency versus harmonic order for different laser strengths a_0. The grating parameters are the same as those in Fig. 3.

It is interesting to apply the prediction of our model to the generation of efficient coherent radiations within the so-called 'water window'. We consider a sufficiently intense KrF pump CP laser normally impacting on the periodic grating target. As the wavelength of the driven laser is 248 nm, the wavelength of the generated 60th harmonic is about 4.1 nm, well within the water-window range (2.3–4.4 nm).[25] For $a_0 = 3.0$ (corresponding to $\sim 1.0 \times 10^{20}\,\mathrm{W/cm^2}$), the efficiency for the 60th harmonic is predicted to be as high as $\eta_{60} \simeq 1.1 \times 10^{-6}$, as shown in Fig. 6. The previous work[25] also suggested that a high-order harmonic could be generated by obliquely irradiating an LP laser pulse on a planar target. The conversion efficiency for the 60th harmonic there was estimated to be 10^{-7}, which is roughly one order lower than that of the grating case at the same laser intensity.

The present scheme for HH radiation depends strongly on the contrast and short duration of the

driving laser pulse. A laser with a long duration or higher intensity can lead to strong heating and expansion, leading to the destruction of the grating surface structure. Fortunately, techniques such as the plasma mirror[26] to achieve an ultrahigh contrast ratio offer the opportunity to extend such studies at very high intensities. The effect of a periodic grating on resonant surface-wave excitation and enhancement of proton acceleration has been experimentally demonstrated in the laser condition of relativistically strong intensity ($>10^{19}$ W/cm^2) and very high contrast ratio ($\sim 10^{-12}$).[27]

In conclusion, based on the surface current model presented in previous works, high order harmonics generated from over-dense plasma grating normally irradiated by a short-pulse ultra-intense circularly polarized laser have been theoretically studied. It is shown that a considerable part of the scattered energy is in the form of higher harmonics in the nonlinear scattering from relativistic electrons movement at the sufficiently strong laser intensity. Due to the interference effect of the grating, these harmonics matching with the grating periodicity are further enhanced and folded into small solid angles with respect to the surface direction. Our results suggest that the availability of laser systems with ultrahigh contrast may allow us to use structured targets for enhanced HHs at the highest intensities available today. It is also demonstrated that coherent water-window x-rays could be efficiently produced using the powerful femtosecond KrF laser technology, which will be available in the future.

References

[1] Ganeev R A, Suzuki M, Baba M and Kuroda H 2009 *Appl. Phys. Lett.* **94** 051101
[2] Krausz F and Ivanov M 2009 *Rev. Mod. Phys.* **81** 163
[3] Cavalieri A L, Müller N, Uphues T et al 2007 *Nature* **449** 1029
[4] Laovorakiat C, Siemens M, Murnane M M et al 2009 *Phys. Rev. Lett.* **103** 257402
[5] Brau C A 1988 *Science* **239** 1115
[6] Andreev N E, Kuznetsov S V, Pogosova A A et al 2003 *Phys. Rev. ST Accel. Beams* **6** 041301
[7] Burza M, Gonoskov A, Svensson K et al 2013 *Phys. Rev. ST Accel. Beams* **16** 011301
[8] Hentschel M, Kienberger R and Spielmann C 2001 *Nature* **414** 509
[9] Kienberger R, Goulielmakis E, Uiberacker M et al 2004 *Nature* **427** 817
[10] Zhang J, Du H, Pan X F et al 2016 *Chin. Phys.* B **25** 113201
[11] Yi L X, Feng L H, Shen L X et al 2016 *Acta Phys. Sin.* **65** 123201 (in Chinese)
[12] Shen L X, Yi L X, Qun W et al 2015 *Acta Phys. Sin.* **64** 193201 (in Chinese)
[13] Bulanov S V, Naumova N M and Pegoraro F 1994 *Phys. Plasmas* **1** 745
[14] Lichters R, Meyer-Ter-Vehn J and Pukhov A 1996 *Phys. Plasmas* **3** 3425
[15] Naumova N M, Nees J A, Sokolov I V et al 2004 *Phys. Rev. Lett.* **92** 063902
[16] Geissler M, Rykovanov S, Schreiber J et al 2007 *New J. Phys.* **9** 218
[17] Mikhailova Y M, Platonenko V T and Rykovanov S G 2005 *JETP Lett.* **81** 571
[18] Baeva T, Gordienko S and Pukhov A 2006 *Phys. Rev.* E **74** 046404
[19] Yu W, Yu M Y, Zhang J and Xu Z 1998 *Phys. Rev.* E **57** R2531
[20] Brownell J H, Walsh J and Doucas G 1998 *Phys. Rev.* E **57** 1075
[21] Liu C S, Tripathi V K, Shao X and Liu T C 2015 *Phys. Plasmas* **22** 023105
[22] Tatjana B and Violeta M 2015 *J. Russ. Laser Res.* **36** 31
[23] Liang Q T 2012 *Advanced Physical Optics* (Beijing: Electronics Industry)
[24] Zhang S J, Zhuo H B, Zou D B et al 2016 *Phys. Rev.* E **93** 053206
[25] Gibbon P 1996 *Phys. Rev. Lett.* **76** 50
[26] Dromey B, Kar S, Zepf M and Foster P 2004 *Rev. Sci. Instrum.* **75** 645
[27] Ceccotti T, Floquet V, Sgattoni A et al 2013 *Phys. Rev. Lett.* **111** 185001